

# A Damage Examination Method by C-Scan on CFRP Laminate

H. S. Chen<sup>1</sup>, W. C. Chen<sup>2</sup>, S. F. Hwang<sup>3</sup>

<sup>1,2</sup>*National Formosa University: Huwei Township, Yunlin County, Taiwan*

<sup>3</sup>*National Yunlin University of Science and Technology: Douliu, Yunlin County, Taiwan*

Because that materials under cyclic loading for a period will present the phenomenon of crack, fatigue or structure failure. This paper aims at the framework of detective process on the experimental fatigue damage growth rate of  $[0^\circ]_8$  CFRP laminates and at development of the corresponding damage growth model. In order not to further damage the structure, a C-Scan examination were carried on the specimens which experience an assigned cycles with the specific load conditions and obtained their related surface scanning images. The purposes of this research are to develop a programmed code with an ability to quantify the fatigue damage of the specimens which undergo any specific stress conditions and to establish data base of the damage growth rate of the compound affected by fatigue stress. With the help of this programmed code, it transferred the scanned images into digital images and used the programmed code to evaluate the damaged level of compound material. The obtained results were used to develop the damage growth rate model of the compound. The comparison between the results of this study and other researches had been done, and the detective process on the quantification of the fatigue damage growth rate and the expectation of the remnant fatigue life of the compound were also completed.

## 1. Introduction

To characterize the fatigue properties of composite materials and to predict their fatigue life are complicated tasks because of the heterogeneity, complexity of the failure modes, multi-failure mechanisms, and damage-related stress redistribution [1]. These complicated properties are due to the factors such as matrix material, fiber material, interfacial structure, volume fractions, fiber orientation, moisture content, porosity, applied stress and strain rate, etc. Consequently, the most current models proposed to characterize the fatigue properties and to predict the fatigue life of composites are empirical.

For the purpose of safety, an employed structure must be inspected if there is how much damage inside the structure caused by fatigue during its service lifetime. The studies of fatigue damage or their accumulation of composite materials are based on the sizes of cracks, delaminations and fiber breaks of the composites under cyclic loadings, practically. For example, in the paper [2] and [3], Reifsnider and Stinchcomb [3] proposed a critical element concept to deduce a non-linear fatigue life prediction methodology for layered composites and to determine the fatigue response (strength) of the composites by way of the microcracks and failure mechanisms. Herakovich et al. [4] developed a three-dimensional finite element analysis model to reveal the transverse cracking problem in cross-ply laminates. Sun et al. [5] utilized Monte Carlo technique to develop a model for predicting the damage development under specific load and

temperature. Dzenis [6-7] adopted a lamination theory and a stochastic mesomechanics approach to develop a novel general model of damage evolution and failure of laminates under cyclic loading. These studies reveal that failure analyses of materials and structures are very important in the fields of experimental mechanics and optical inspection. However, it is regrettable that there is little straightforward evidence to describe the mechanism and history of crack growth. Because that the bulk of fatigue elements can still be in service, the non-destructive evaluation method utilized to inspect the fracture level of a structure is necessary. Since, ultrasound detecting method can examine the defects existing within material. Using ultrasound detecting flaw method to study the history of crack growth is a good ideal. By careful analysis of the image and information obtained from the ultrasound detection, we are able to figure out the damage inside the composite material. With the verification of experiments aided by the image processing techniques, this will contribute to building a fatigue damage model and secure the life prediction and designing safety of composite material. Digital image correlation method (DIC) is a good non-destructive evaluation method utilized to quantify the fatigue damage level of a structure. The employment of DIC in building an estimate model on the overall fatigue damage growth of composite materials will enable us to have understanding of their fatigue damage history. Thus, a larger, faster and safer application of composite materials can be expected.

The study mainly aims to apply the digital image processing techniques to building an integrated fatigue damage growth model for composite materials. Another aim of this study is trying to design an empirical prediction system to detect the fatigue damage of carbon-fiber composite materials by the combination of digital image processing techniques with C-Scan analysis. We build an effective carbon-fiber composite materials fatigue damage prediction model by using the estimate system as well as the damage level after the different assigned fatigue cyclic loading conditions mentioned above.

## **2.Experimental Details**

The fatigue tests of unidirectional specimens made of UD-12K/Carbon/FAW125 epoxy composites are conducted at room temperature under different stress levels, stress frequencies, and stress ratios. The angle of the unidirectional composite specimens is  $0^\circ$  and was made by 8 layers of prepregs. The geometry of the specimen and its dimensions are shown in Fig. 2.1. The end tabs are glass/epoxy material with 2.0 mm thickness. The average material properties of carbon composite are listed in Table 2.1. All the fatigue tests were conducted at a Shimadzu servo-hydraulic testing machine controlled by a Shimadzu winservo system. The tests were under the conditions of load control with a sinusoidal waveform. The stress ratio here is defined as the ratio of the minimum stress to the maximum stress in a sinusoidal load waveform. In considering the effect of stress frequency, the stress frequencies tested are 3Hz, 5Hz, and 10Hz, when the stress ratio is fixed as 0. In considering the effect of stress ratio, the stress frequencies were 8Hz, and the stress ratios were 0.1, 0.3, and 0.5. At each stress frequency or stress ratio, the stress levels are 0.6 times of the strength of the composites. In considering the effect of stress level, the stress frequencies were fixed as 8Hz, and the stress ratios were fixed as 0.3, and stress level were 0.5 and 0.6 times of the strength of the composites. The specimens were inspected by C-Scan after signed loading cycles with specific load conditions and then the other signed loading cycles with the same specific load conditions were applied to

these specimens, sequentially. And the result images obtained from the tests of C-Scan were translated to digital data by DIC method to evaluate the fatigue damage level.

### 3. Fatigue Damage Model

It was proved that fatigue frequency ( $f$ ) and stress ratio ( $R$ ) could change fatigue life [9-12]. It should be interesting to apply this aspect in fatigue damage model. For this purpose, a damage model considering the effects of  $R$  and  $f$  was developed to describe the phenomenon of the evolution of damage area on FRP coupon during cyclic loading history. And the preceding mentioned fatigue tests data were utilized to evaluate the model parameters. In order to describe this crack growth, we define  $D(n)$  as a quantitative index of the fatigue damage, which is linearly dependent on the existent damage area in the coupon. These digital damage data of the specimens were obtained by the C-Scan images and DIC method. From the viewpoint of fracture mechanics, under a specific loading condition, the quantity of  $D(n)$  would affect the growth rate of  $D(n)$ , and then it is supposed that the growth rate of the  $D(n)$  is proportional to the damage index  $D(n)$ . Then the governing equation is

$$\frac{d D(n)}{d n} = D(n) (a - b D(n)) \quad (1)$$

where  $a$  and  $b$  are undecided constants. To solve this equation and introduce  $D(n) = 1$  when  $n$  approaches infinite. Moreover,  $D(n)$  may be affected by the fatigue stress level, stress ratio and stress frequency. Hence, there is a correction factor should be introduced into equation in terms of these factors as the form of  $A_2 (S/\sigma_u, f, R)$ . This comes to Equation (2),

$$D(n) = A_2 \left( \frac{S}{\sigma_u}, f, R \right) \times \frac{1}{1 + \frac{1}{ac} \times e^{-an}} \quad (2)$$

where  $c$  is an integral constant and the stress level  $S$  is defined as the maximum loading stress and  $\sigma_u$  is the static tensile strength of the material. Let  $A(S/\sigma_u, f, R) = 1/ac$ . Then Equation (2) could be expressed as the following form

$$D(n) = A_2 \left( \frac{S}{\sigma_u}, f, R \right) \times \frac{1}{1 + A \left( \frac{S}{\sigma_u}, f, R \right) \times e^{-an}} \quad (3)$$

The function  $A_2 (S/\sigma_u, f, R)$  and  $A(S/\sigma_u, f, R)$  can be obtained by the evaluated fatigue damage level from digital data of DIC method.

### 4. Results and Discussion

Figures 4.1-4.3 are the C-San images of a composite specimen after specific fatigue cycles under the conditions of 3Hz, 5Hz, 10Hz stress frequency, respective. The other loading conditions are 0 stress ratio, and 0.6 times of the strength of the composites. From the images 4.1(a) – 4.1(f), the colors change from yellow to green in the images reveals that the locations and areas of damage level, and the total areas of these defects increase with the colors change of yellow to green when the loading cycles increase. Different colors in the images reveal different fatigue damage. Red area reveals light damage and green area means that there are more defects inside the zone. The character

of the different damage level appears different color in the C-Scan image can be utilized to be the damage index of the specimen under fatigue loading. By estimating the rate of each color, the damage level is obtained. In order to evaluate the damage level by way of the color ratio, a programmed code was developed in this study. By Figures 4.1-4.3 and the code, a series of plots of damage index of the specimens' vs. fatigue life were completed. The results are shown in Figures 4.4-4.6. from these figures and other results of different corresponding tests with specific loading conditions, the parameters of equation (3) were decided. The results are shown in Figures 4.7-4.15. By regressive method, the parameters, A, A<sub>2</sub> and a are obtained and shown as equation (4) - equation (6).

$$\begin{aligned}
 & A(f, R, (\frac{S}{\sigma_u})) \\
 &= (0.014651 - \frac{0.0128}{1 + e^{(f-6.1411)/1.3855}}) \\
 &\times (0.011411 - \frac{0.00552}{1 + e^{(R-0.24163)/0.049231}}) \\
 &\times (-0.0294 + 0.0704(\frac{S}{\sigma_u}))
 \end{aligned} \tag{4}$$

$$\begin{aligned}
 & A_2(f, R, (\frac{S}{\sigma_u})) \\
 &= (0.28747 + \frac{0.04044}{1 + e^{(f-4.5934)/0.66705}}) \\
 &\times (0.34378 + \frac{0.05208}{1 + e^{(R-0.35856)/0.050536}}) \\
 &\times (0.14983 + 0.5666(\frac{S}{\sigma_u}))
 \end{aligned} \tag{5}$$

$$\begin{aligned}
 & a(f, R, (\frac{S}{\sigma_u})) \\
 &= (1.4240 + \frac{1.5017}{1 + e^{(f-4.9807)/0.66082}}) \\
 &\times (1.5848 - \frac{0.3318}{1 + e^{(R-0.24686)/0.063384}}) \\
 &\times (4.13182 - 4.12832(\frac{S}{\sigma_u}))
 \end{aligned} \tag{6}$$

## 5. Conclusion

This study has shown that C-Scan inspection and DIC method can be combined to detect and to quantify the damage of an element under cyclic loading. A non-destructive evaluation model utilized to inspect the fatigue damage level of a specimen is developed. This model estimates the fatigue damage level by C-Scan and DIC method, and these damage data can be utilized to decide the parameters of Equation (3), which can be used to predict damage level of the specimen with specific loading conditions. Especially, this model displays a straightforward method to describe the mechanism and history of fatigue damage growth of a composite material. A damage index was defined by the color ratio of a C-Scan image. The sigmoid curves of the damage index vs. fatigue life are shown in the results. And the mathematic functions of the curves with specific fatigue

load conditions are obtained in this study.

### Reference

- [1] G. Shen, Fatigue Life Prediction of Composite Based on Microstress Analysis, PhD thesis, University of Waterloo, 1993.
- [2] K.L. Reifsnider, K. Schulte, J.C. Duke, Long-Term Fatigue Behavior of Composite Materials, Long-Term Behavior of Composites, ASTM STP 813, T. K. O'Brien (Eds.), American Society for Testing and Materials, Philadelphia, 1983, pp.136-159.
- [3] K.L. Reifsnider, W.W. Stinchcomb, A Critical-Element Model of the Residual Strength and Life of Fatigue-Loaded Composite Coupons, Composites materials, fatigue and fracture, ASTM STP 907, Hahn HT (Eds.), American Society for Testing and Materials, Philadelphia (PA), 1986, pp.298-313.
- [4] C.T. Herakovich, J. Aboudi, S.W. Lee, E.A. Strauss, Damage in Composite Laminates: Effects of Transverse Cracks, Mechanics of Materials **7** (1988) 91-107.
- [5] Z. Sun, I.M. Daniel, J.J. Luo, Progresses in Fracture and Strength of Materials and Structures, Materials Science and Engineering A **361**,(2003) 302.
- [6] Y.A. Dzenis, Cycle-based analysis of damage and failure in advanced composites under fatigue: 1. Experimental observation of damage development within loading cycles, International Journal of Fatigue **25** (6) (2003) 499-510.
- [7] Y.A. Dzenis, Cycle-based analysis of damage and failure in advanced composites under fatigue: 2. Stochastic mesomechanics modeling, International Journal of Fatigue **25**(6) (2003) 511-520.
- [8] Z.F. Zhang, Y.L. Kang, H.W. Wang, Q.H. Qin, Y. Q., X.Q. Li, A novel coarse-fine search scheme for digital image correlation method, Measurement **39** (2006) 710-718.
- [9] X.R. Xiao, Modeling of Load Frequency Effect on Fatigue Life of Thermoplastic Composites, Journal of Composite Materials **33** (12) (1999) 1141-1158.
- [10] J.F. Mandell, U. Meier, Effects of Stress Ratio, Frequency, and Loading Time on the Tensile Fatigue of Glass-Reinforced Epoxy, Long-Term Behavior of Composites, ASTM STP 813, T. K. O'Brien (Eds.), American Society for Testing and Materials, 1983, pp. 55-77.
- [11] J. A. Epaarachchi, P.D. Clausen, An Empirical Model for Fatigue Behavior Prediction of Glass Fiber-Reinforced Plastic Composites for Various Stress Ratio and Testing Frequencies, Composites Part A: Applied Science and Manufacturing **34** (2003) pp.313-326.
- [12] Y. Miyano, M.K. McMurray, Loading Rate and Temperature Dependence on Flexural Fatigue Behavior of a Satin Woven CFRP Laminate, Journal of Composite Materials **28** (13) (1994) 1250-1260.

Table 2.1. Mechanical property of carbon/epoxy composites

$E_{11}$ (GPa)	$X$ (MPa)	$V_f$	$\epsilon_{1f}$
145.08	1899.62	0.63	1.36%

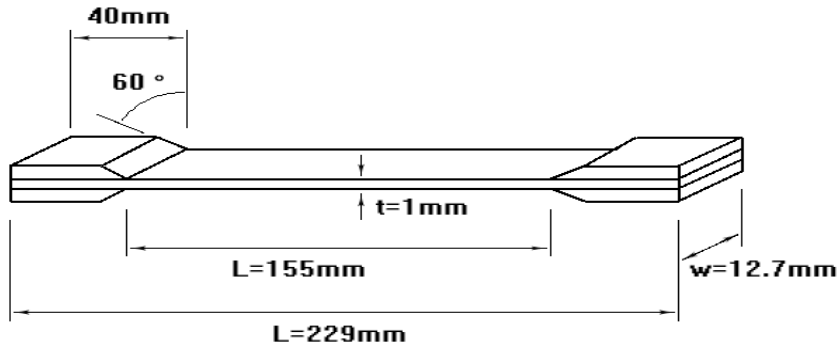


Fig. 2.1. The geometry and dimension of the specimen.

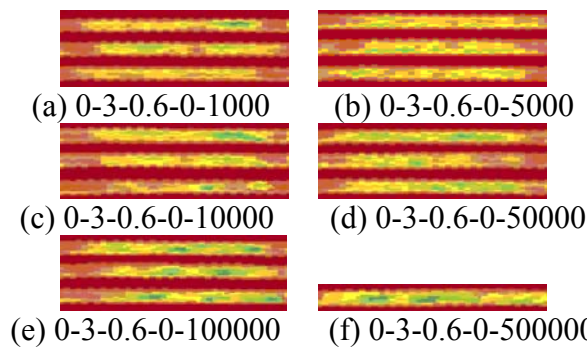


Fig.4.1 These images were obtained by C-Scan. The serial number, 0-3-0.6-0-xxxx, means that the sequence tests for a  $0^\circ$  carbon specimen under the stress frequency 3Hz, the stress level 0.6 times of the strength of the composite, the stress ratio 0, and after xxxx loading cycles.

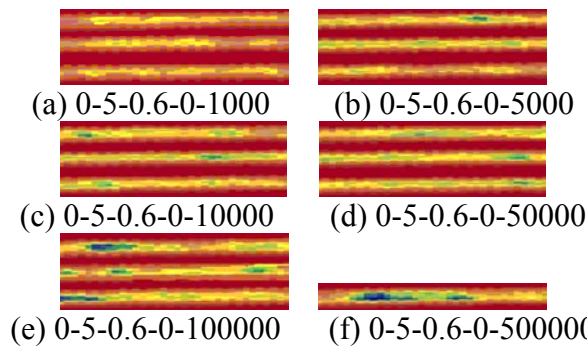
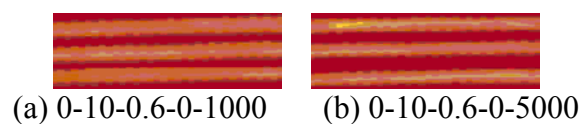


Fig.4.2 These images were obtained by C-Scan. The serial number, 0-5-0.6-0-xxxx, means that the sequence tests for a  $0^\circ$  carbon specimen under the stress frequency 5Hz, the stress level 0.6 times of the strength of the composite, the stress ratio 0, and after xxxx loading cycles



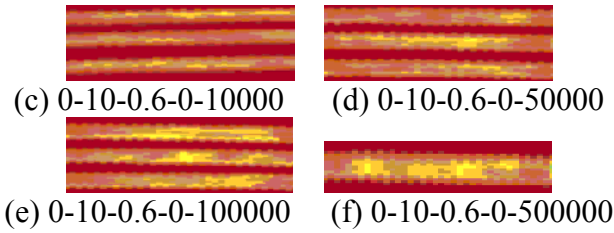


Fig.4.3 These images were obtained by C-Scan. The serial number, 0-3-0.6-0-xxxx, means that the sequence tests for a  $0^\circ$  carbon specimen under the stress frequency 10Hz, the stress level 0.6 times of the strength of the composite, the stress ratio 0, and after xxxx loading cycles

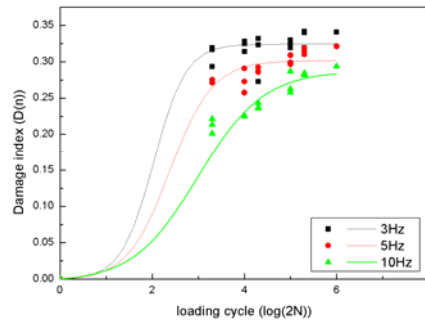


Fig.4.4 The relationship of damage index vs. loading cycles of the CFRP coupons with the loading conditions of  $R = 0.3$ ,  $(S/\sigma_u) = 0.6$ ,  $f=3, 5$  and 10Hz.

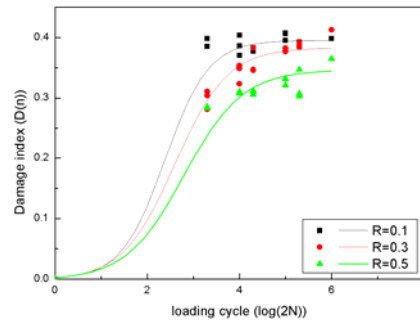


Fig.4.5 The relationship of damage index vs. loading cycles of the CFRP coupons with the loading conditions of  $f=8$ Hz,  $(S/\sigma_u) = 0.6$ ,  $R = 0.1, 0.3$  and 0.5.

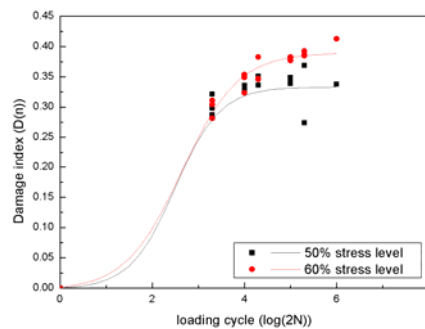


Fig.4.6 The relationship of damage index vs. loading cycles of the CFRP coupons with the loading conditions of  $f = 8\text{Hz}$ ,  $R = 0$ ,  $(S/\sigma_u) = 0.5$  and  $0.6$ .

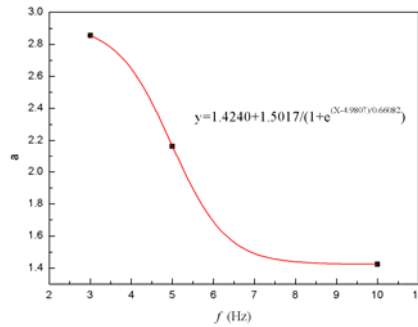


Fig.4.7 The relationship of  $a$  vs.  $f$  of the CFRP coupons with the loading conditions of  $R = 0.3$ ,  $(S/\sigma_u) = 0.6$ ,  $f = 3, 5$  and  $10\text{Hz}$ .

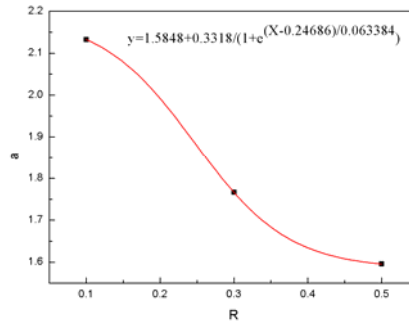


Fig.4.8 The relationship of  $a$  vs.  $R$  of the CFRP coupons with the loading conditions of  $f = 8\text{Hz}$ ,  $(S/\sigma_u) = 0.6$ ,  $R = 0.1, 0.3$  and  $0.5$ .

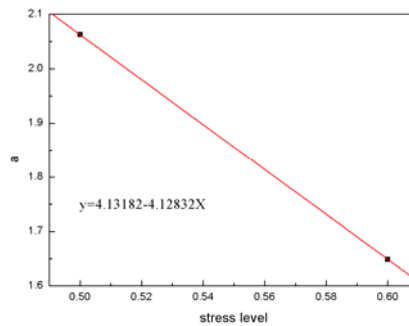


Fig.4.9 The relationship of  $a$  vs. stress level of the CFRP coupons with the loading conditions of  $f = 8\text{Hz}$ ,  $R = 0$ ,  $(S/\sigma_u) = 0.5$  and  $0.6$ .

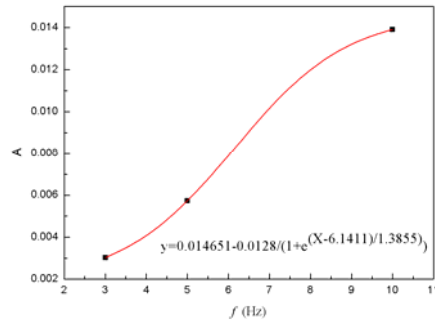


Fig.4.10 The relationship of  $A$  vs.  $f$  of the CFRP coupons with the loading conditions of  $R = 0.3$ ,  $(S/\sigma_u) = 0.6$ ,  $f = 3, 5$  and  $10\text{Hz}$ .

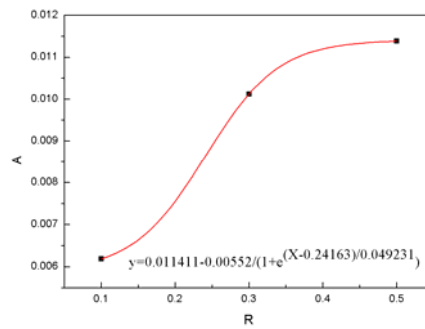


Fig.4.11 The relationship of  $A$  vs.  $R$  of the CFRP coupons with the loading conditions of  $f = 8\text{Hz}$ ,  $(S/\sigma_u) = 0.6$ ,  $R = 0.1, 0.3$  and  $0.5$ .

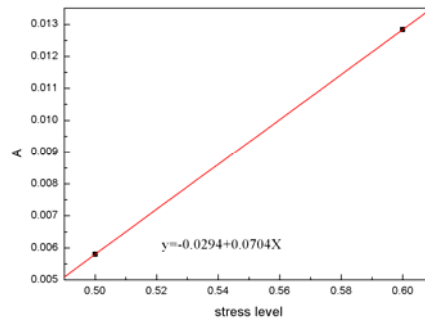


Fig.4.12 The relationship of  $A$  vs. stress level of the CFRP coupons with the loading conditions of  $f = 8\text{Hz}$ ,  $R = 0$ ,  $(S/\sigma_u) = 0.5$  and  $0.6$ .

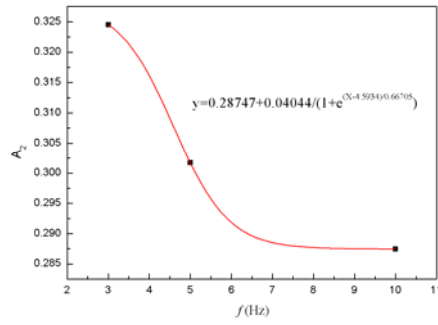


Fig.4.13 The relationship of  $A_2$  vs.  $f$  of the CFRP coupons with the loading conditions of  $R = 0.3$ ,  $(S/\sigma_u) = 0.6$ ,  $f = 3, 5$  and  $10\text{Hz}$ .

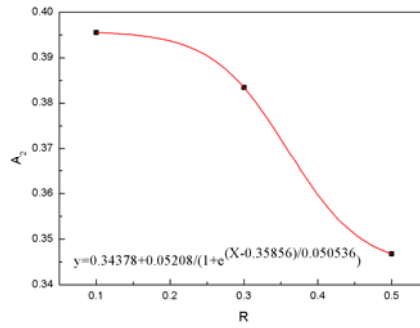


Fig.4.14 The relationship of  $A_2$  vs.  $R$  of the CFRP coupons with the loading conditions of  $f = 8\text{Hz}$ ,  $(S/\sigma_u) = 0.6$ ,  $R = 0.1, 0.3$  and  $0.5$ .

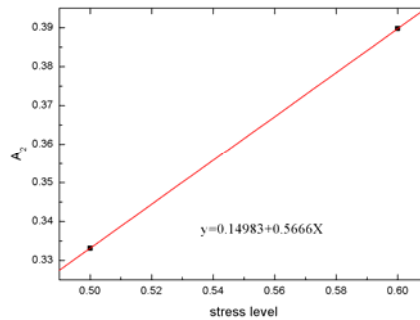


Fig.4.15 The relationship of  $A_2$  vs. stress level of the CFRP coupons with the loading conditions of  $f = 8\text{Hz}$ ,  $R = 0$ ,  $(S/\sigma_u) = 0.5$  and  $0.6$ .